

## Transfer of coherent dynamics between discrete excitons and exciton Fano continua in quantum wells

S. Arlt, J. Kunde, F. Morier-Genoud, U. Keller, and U. Siegner

*Swiss Federal Institute of Technology Zurich, Institute of Quantum Electronics, ETH Honggerberg HPT, CH-8093 Zurich, Switzerland*

(Received 23 February 2000)

Four-wave-mixing in semiconductor quantum wells with spectrally shaped broadband laser pulses demonstrates that the coherent dynamics of discrete excitons can be detected in the coherent emission from exciton Fano continua and vice versa. In particular, quantum beating between discrete heavy and light hole excitons is observed in the coherent emission from the continuum. The results can be understood in a common ground-state picture of strongly coupled transitions. This model shows that the transfer of the amplitude of the nonlinear coherent polarization is at the origin of the experimental results.

In semiconductors, interactions between energetically nondegenerate optical excitations can play an important role in the coherent regime.<sup>1-4</sup> These interactions have their origin in excitation-induced dephasing.<sup>2,5,1</sup> A powerful tool for the experimental study of nondegenerate coherent interactions is partially nondegenerate (PND) four-wave mixing (FWM).<sup>2</sup> In a PND-FWM experiment, one applies two excitation laser pulses with only partially overlapping spectra and analyzes the coherent emission from transitions that have only been excited by one of the two excitation pulses. The PND-FWM technique has been used to study nondegenerate coherent interactions between the discrete exciton and unstructured continuum transitions of the same subband in quantum wells.<sup>2</sup> In these experiments, coherent emission from the exciton has been generated due to the excitation of continuum transitions, proving the existence of strong nondegenerate coherent interactions.<sup>2</sup> The PND-FWM technique has also been applied to study nondegenerate coherent interactions between discrete quasi-zero-dimensional magnetoexcitons in quantum wells<sup>2</sup> and between discrete excitons in inhomogeneously broadened ensembles.<sup>6</sup>

In degenerate FWM experiments, strong coupling has been observed between discrete excitons and exciton Fano continua.<sup>7,4</sup> Thus, these systems are well suited to explore the consequences of strong nondegenerate coherent interactions with the PND-FWM technique. In this paper, we report on the PND-FWM studies of discrete excitons and exciton Fano continua in quantum wells. We analyze the dynamics using a complete set of four PND-FWM traces, i.e., we measure the dynamics at the discrete excitons and in the continuum for two different excitation conditions. These data show that the coherent dynamics of discrete excitons can be detected in the coherent emission from exciton Fano continua and vice versa. In particular, this transfer of coherent dynamics allows for the observation of the quantum beating between the discrete heavy and light hole excitons<sup>8,9</sup> if coherent emission from the continuum is detected. The transfer of coherent dynamics in PND-FWM can generate coherent radiation from the continuum that is absent in degenerate FWM. Earlier work<sup>2,4,7,10,11,3</sup> only demonstrated the suppression of excitonic coherent emission due to interaction with continuum transitions. Thus, our results give new insight into the consequences of non-degenerate coherent interactions in semiconductors.

Our results can be understood if the discrete exciton and the Fano continuum transitions are modeled as a multitude of excited states coupled to a common ground state.<sup>2</sup> This model is based on the strong nondegenerate coherent interactions between exciton and continuum transitions.<sup>2</sup> We will argue that the transfer of the amplitude of the nonlinear coherent polarization is at the origin of the experimental findings. The amplitude of the nonlinear coherent polarization determines the dynamical evolution of transient FWM signals in the time delay domain, in which the transfer of coherent dynamics is observed.

We have performed transient FWM experiments in the standard two-beam configuration with parallel polarized laser pulses with wave vectors  $\mathbf{k}_1$  and  $\mathbf{k}_2$ . The FWM signal, in direction  $2\mathbf{k}_2 - \mathbf{k}_1$ , is measured either temporally and spectrally integrated versus time delay  $\Delta t$  between the excitation laser pulses or spectrally resolved at fixed time delays  $\Delta t$ . A Ti:sapphire laser generates 16 fs pulses with a 82 meV wide spectrum (full width at half maximum, FWHM) centered at 1.55 eV. The laser pulse with wave vector  $\mathbf{k}_1$  is passed through a spectral amplitude filter, which consists of two SF 10 prisms in double-path configuration and an adjustable slit.<sup>12</sup> This setup allows us to change the center wavelength and the FWHM of pulse spectrum  $\mathbf{k}_1$ . In all experiments, the filtered narrow-band pulses  $\mathbf{k}_1$  have a spectral FWHM of about 9 meV and a temporal width of about 200 fs. The pulse with wave vector  $\mathbf{k}_2$  is not spectrally filtered. This experimental scheme is referred to as PND-FWM.<sup>2</sup>

The PND-FWM experiments were performed on a GaAs/Al<sub>0.3</sub>Ga<sub>0.7</sub>As multiple quantum well with 160 Å wells and 150 Å barriers, repeated 30 times. To allow for transmission experiments, the sample was glued on a sapphire disk and the GaAs substrate was removed by chemical wet etching. The sample is antireflection coated at the front side. All experiments have been performed at 10 K.

Figure 1 shows the linear absorption spectrum of the multiple quantum well and the broadband and narrow-band laser spectra. The absorption spectrum comprises heavy hole (hh) and light hole (lh) excitonic transitions corresponding to different electron ( $e$ ) and hole subbands with subband index  $n$ . The  $e(n=1)$ hh( $n=1$ ) exciton transition at 1.528 eV has a FWHM of 1.0 meV, demonstrating small inhomogeneous

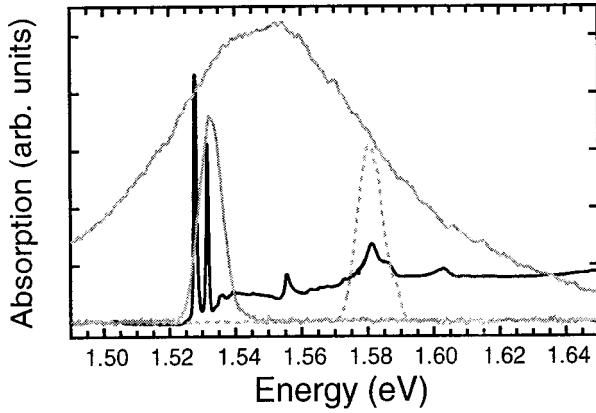


FIG. 1. Linear absorption spectrum (black-solid line) of the quantum well sample at 10 K. Spectrum of the broadband laser pulse  $k_2$  (gray-solid line) exciting all resonances. Spectrum of the narrow-band laser pulse  $k_1$  exciting either the  $e1hh1/e1lh1$  excitonic resonances (gray-solid line) or the  $e2hh2$  exciton Fano continuum (gray-dashed line).

broadening in this high-quality sample. The other resonances can be assigned to the  $e1lh1$  (at 1.5315 eV), the  $e1hh3$  (at 1.556 eV), the  $e2hh2$  (at 1.581 eV), and the  $e2lh2$  (at 1.603 eV) excitonic transitions. The broadband laser pulse  $k_2$  excites all these transitions while the narrow-band pulse  $k_1$  selectively excites either the  $e1hh1/e1lh1$  or the  $e2hh2$  transition, as shown in Fig. 1. In all experiments, pulse  $k_2$  produces a pulse energy fluence of  $2.1 \mu\text{J}/\text{cm}^2$ , whereas the fluences of pulse  $k_1$  are  $0.18 \mu\text{J}/\text{cm}^2$  and  $0.17 \mu\text{J}/\text{cm}^2$  at the  $e1hh1$  and  $e2hh2$  resonances, respectively.

Note that the higher-order excitons, such as  $e2hh2$ , are coupled to the energetically degenerate continua of lower-order subband pairs and form exciton Fano continua.<sup>13,14,15</sup> In degenerate FWM experiments, exciton Fano continua generate a FWM signal only if the excitation pulses overlap in time, leading to a pulse width limited FWM trace vs time delay  $\Delta t$ .<sup>4,16</sup> This behavior is not related to dephasing but has its origin in many-body exciton-continuum coupling.<sup>3,4,10</sup> In contrast, the FWM signal of the discrete  $e1hh1$  and  $e1lh1$  excitons is determined by dephasing and quantum beating<sup>8,9</sup> in the  $\Delta t$  domain. This allows one to assign the FWM dynamics to either the discrete  $e1hh1/e1lh1$  excitons or to the exciton Fano continua.

In Fig. 2 we compare spectrally resolved PND-FWM signals at fixed time delays  $\Delta t$  corresponding to the maximum of the FWM emission. In Fig. 2(a) the narrow-band pulse  $k_1$  excites the  $e2hh2$  exciton Fano continuum. FWM signals are emitted at the  $e1hh1$  and  $e1lh1$  discrete exciton resonances and at the spectral positions of the  $e1hh3$  and  $e2hh2$  exciton Fano continua. The  $e1hh1$  emission dominates the FWM spectrum although the  $e1hh1$  exciton is not excited by the narrow-band laser pulse  $k_1$ . We refer to coherent emission as “indirect emission” if only the broadband pulse  $k_2$  has frequency components at the spectral position of the emission. By the same token, “direct emission” is generated if both pulses  $k_1$  and  $k_2$  have frequency components at the spectral position of the emission.

Strong indirect emission at the lowest exciton resonance was observed in Ref. 2 if an unstructured continuum without embedded excitons was excited by the narrow-band laser

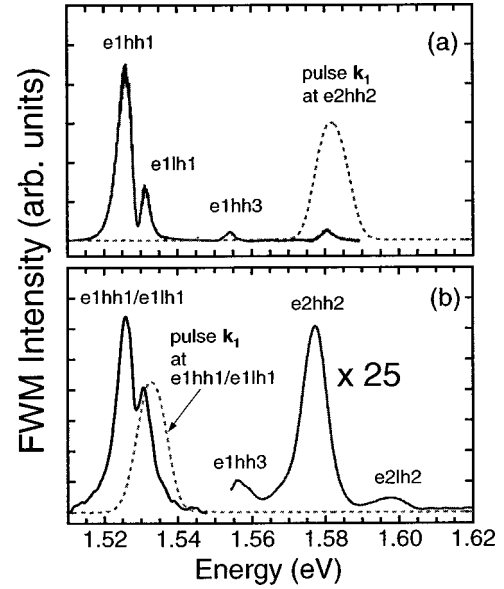


FIG. 2. Spectrally resolved four-wave-mixing signal (solid line) for narrow-band laser pulse  $k_1$  excitation (dashed line) at the  $e2hh2$  exciton Fano continuum (a), and at the  $e1hh1/e1lh1$  discrete exciton resonances (b). The emission signal around the  $e2hh2$  exciton Fano continuum in (b) has been multiplied by a factor of 25. All data are taken at time delays corresponding to the maximum FWM emission.

pulse. This observation demonstrated strong interaction between nondegenerate interband transitions in the coherent regime. Direct emission from the unstructured continuum was not observed in Ref. 2. In Fig. 2(a), we observe both direct and indirect emission. This is due to the large oscillator strength of exciton resonances<sup>17</sup> that are inherently involved in a Fano continuum.

Figure 2(b) shows the spectrally resolved PND-FWM signal if the narrow-band pulse  $k_1$  excites the discrete excitons  $e1hh1$  and  $e1lh1$ . Coherent emission from all resonances between the band-edge and the  $e2hh2$  exciton Fano continuum is observed. Figure 2(b) demonstrates that nondegenerate coherent interactions can generate indirect coherent emission from continuum transitions.

The temporal evolution of the direct and indirect coherent emission in the time delay domain is shown in Fig. 3 for excitation with the narrow-band pulse  $k_1$  at  $e2hh2$  (a) or  $e1hh1/e1lh1$  (b). The FWM emission has been integrated over a 25 meV wide spectral window centered either at the  $e1hh1$  or the  $e2hh2$  resonance. The spectral windows are defined by interference filters whose transmission characteristics ensure that the coherent emission from the different transitions is measured separately. The dashed (thick solid) lines in Figs. 3(a) and 3(b) show the coherent emission around the  $e2hh2$  ( $e1hh1$ ) resonance. For excitation at  $e2hh2$ , the FWM traces at both emission positions show a pulse width limited decay, characteristic for exciton Fano continua. In contrast, for excitation at  $e1hh1/e1lh1$ , the decay of the FWM signal at positive time delays is well resolved at both detection positions, as shown in Fig. 3(b). Moreover, for excitation at the band edge, we observe a pronounced beating modulation for detection around  $e1hh1$  and  $e2hh2$ . The beat detected around  $e1hh1$  can be fitted with a beat period of 1.14 ps, which well matches the energy split-

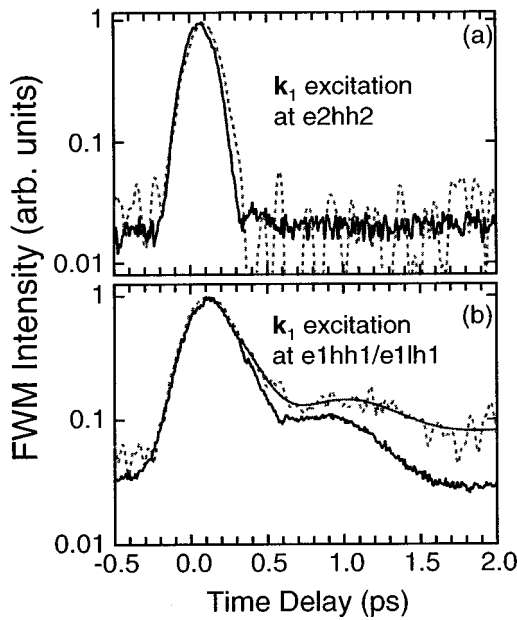


FIG. 3. (a) Temporally integrated four-wave-mixing signal vs time delay for narrow-band laser pulse  $\mathbf{k}_1$  excitation at the  $e2hh2$  exciton Fano continuum (a) or at the  $e1hh1/e1lh1$  discrete exciton resonances (b). Thick-solid lines: coherent emission at the  $e1hh1/e1lh1$  exciton resonances. Dashed lines: coherent emission at the  $e2hh2$  exciton Fano continuum. The thin-solid line in (b) is a fit to the dashed curve (see text).

ting of 3.5 meV between the  $e1hh1$  and  $e1lh1$  discrete exciton resonances seen in linear absorption. Consequently, for excitation and detection around  $e1hh1$ , the hh-lh beating of the lowest excitons is observed, characteristic for the coherent dynamics of these discrete exciton transitions.<sup>8,9</sup>

The thin-solid line in Fig. 3(b) shows a fit to the dashed curve (emission at  $e2hh2$ ) with the beat period of 1.14 ps, taken from the fit to the emission detected around  $e1hh1$  in Fig. 3(b). The excellent agreement between the FWM trace detected at  $e2hh2$  and the fit shows that the hh-lh beat of the lowest-exciton transitions is observed at the spectral position of the  $e2hh2$  Fano continuum. Moreover, for excitation at  $e1hh1$ , the direct and the indirect coherent emission show very similar decay times of 0.32 and 0.40 ps, respectively.

Figure 3 clearly demonstrates that the coherent dynamics of the discrete excitons can be detected in the coherent emission from exciton Fano continua [Fig. 3(b)] and vice versa [Fig. 3(a)]. Due to this transfer of coherent dynamics, indirect coherent emission from the exciton Fano continuum can be generated at time delays larger than the pulse width, which is impossible for direct emission.<sup>4,16</sup>

The transfer of coherent dynamics between discrete exciton transitions and exciton Fano continua in PND-FWM can be understood in the common ground-state picture of strongly interacting transitions. This model was put forward to explain the generation of indirect coherent emission in semiconductors.<sup>2</sup> We will argue that the transfer of the amplitude of the nonlinear coherent polarization is at the origin of the experimental results of Fig. 3. For convenience, in the following we assume that inhomogeneous broadening can be neglected.

In a PND-FWM experiment, the narrow-band pulse  $\mathbf{k}_1$

can create a population grating together with that part of the broadband spectrum of pulse  $\mathbf{k}_2$ , which overlaps with the spectrum of  $\mathbf{k}_1$ . A population grating is created if permitted by the coherence properties of the transitions excited by pulse  $\mathbf{k}_1$ , e.g., if the polarization excited by pulse  $\mathbf{k}_1$  has not yet dephased when pulse  $\mathbf{k}_2$  is applied. If so, the pulses  $\mathbf{k}_1$  and  $\mathbf{k}_2$  create a population grating in the ground state and in the excited states with an energy matched to the photon energies in the  $\mathbf{k}_1$  spectrum.<sup>18,19</sup> In the common ground-state model, all frequency components in the broadband spectrum  $\mathbf{k}_2$  can couple to the population grating in the ground state. Therefore, pulse  $\mathbf{k}_2$  can generate nonlinear polarization in third order in the electric field at transitions involving excited states that have not been excited by pulse  $\mathbf{k}_1$ . This third-order polarization gives rise to a coherent emission that is frequency shifted with respect to the spectrum of  $\mathbf{k}_1$ .<sup>20</sup> This coherent emission constitutes the indirect emission. For inhomogeneously broadened systems, a similar mechanism has been discussed in the context of accumulated<sup>21</sup> and two-color photon echoes.<sup>22</sup>

The strength of the population grating determines the amplitude of the third-order polarization directly after pulse  $\mathbf{k}_2$  has been applied and, therefore, the amplitude  $A$  of the indirect coherent emission, i.e., its maximum value in real time.<sup>18,19</sup> The strength of the population grating is determined by the coherence properties of the transitions excited by pulse  $\mathbf{k}_1$ . For example, the population grating will be weak if the polarization of these transitions rapidly dephases. As a consequence, the coherence properties of the transitions excited by pulse  $\mathbf{k}_1$  determine the amplitude of the third-order polarization and the amplitude  $A$  of the indirect coherent emission, independent of the coherence properties of the emitting transitions. In this way, coherence properties are transferred between spectrally separated transitions. Note that the amplitude of the third-order polarization and the amplitude  $A$  of the indirect coherent emission depend on the time delay  $\Delta t$  between the pulses  $\mathbf{k}_1$  and  $\mathbf{k}_2$ :  $A=A(\Delta t)$ .

In real time  $t$ , the emitting transitions determine the decay of the indirect coherent emission and, in turn, its spectrum. Therefore, for excitation around  $e1hh1$ , the beating seen in the time delay domain around the  $e2hh2$  exciton Fano continuum in Fig. 3(b) is not reflected by an energy splitting in the spectrum around the  $e2hh2$  exciton Fano continuum in Fig. 2(b). The decay of the indirect coherent emission in real time  $t$  is independent of the amplitude  $A$ . Therefore, one can write for the indirect coherent emission  $S(t, \Delta t) = A(\Delta t)f(t)$ , where  $f(t)$  describes the real-time decay determined by the emitting transitions. If  $S(t, \Delta t)$  is temporally integrated and plotted vs time delay  $\Delta t$ ,  $f(t)$  only determines the height of this curve whereas the shape is solely determined by  $A(\Delta t)$ . As a consequence, the transfer of coherence properties between spectrally separated transitions is observed as a transfer of coherent dynamics in the  $\Delta t$  domain, as demonstrated for discrete exciton transitions and exciton Fano continua in Fig. 3.

We like to emphasize that the transfer of coherent dynamics based on the described mechanism should be observable in any multilevel system with a common ground state. In these systems, PND-FWM can be used to detect the coherent

dynamics of one set of transitions in the emission from other ones.

In conclusion, partially nondegenerate four-wave-mixing experiments in a semiconductor quantum well show that the coherent dynamics of discrete excitons can be detected in the

coherent emission from exciton Fano continua and vice versa. This result sheds light on the consequences of strong nondegenerate coherent interactions in semiconductors.

This work was supported by the Swiss National Science Foundation.

- 
- <sup>1</sup>T. Rappen, U.-G. Peter, M. Wegener, and W. Schäfer, *Phys. Rev. B* **49**, 10 774 (1994).
- <sup>2</sup>S. T. Cundiff, M. Koch, W. H. Knox, J. Shah, and W. Stolz, *Phys. Rev. Lett.* **77**, 1107 (1996).
- <sup>3</sup>K. El Sayed, D. Birkedal, V. G. Lyssenko, and J. M. Hvam, *Phys. Rev. B* **55**, 2456 (1997).
- <sup>4</sup>S. Arlt, U. Siegner, F. Morier-Genoud, and U. Keller, *Phys. Rev. B* **58**, 13 073 (1998).
- <sup>5</sup>H. Wang, K. Ferrio, D. G. Steel, Y. Z. Hu, R. Binder, and S. W. Koch, *Phys. Rev. Lett.* **71**, 1261 (1993).
- <sup>6</sup>A. Euteneuer, E. Finger, M. Hofmann, W. Stolz, T. Meier, P. Thomas, S. W. Koch, W. W. Rühle, R. Hey, and K. Ploog, *Phys. Rev. Lett.* **83**, 2073 (1999).
- <sup>7</sup>U. Siegner, M.-A. Mycek, S. Glutsch, and D. S. Chemla, *Phys. Rev. B* **51**, 4953 (1995).
- <sup>8</sup>B. F. Feuerbacher, J. Kuhl, R. Eccleston, and K. Ploog, *Solid State Commun.* **74**, 1279 (1990).
- <sup>9</sup>K. Leo, T. C. Damen, J. Shah, E. O. Göbel, and K. Köhler, *Appl. Phys. Lett.* **57**, 19 (1990).
- <sup>10</sup>M. U. Wehner, D. Steinbach, and M. Wegener, *Phys. Rev. B* **54**, R5211 (1996).
- <sup>11</sup>D. Birkedal, V. G. Lyssenko, J. M. Hvam, and K. ElSayed, *Phys. Rev. B* **54**, R14 250 (1996).
- <sup>12</sup>R. L. Fork, *Opt. Lett.* **11**, 629 (1986).
- <sup>13</sup>D. Y. Oberli, G. Böhm, G. Weimann, and J. A. Brum, *Phys. Rev. B* **49**, 5757 (1994).
- <sup>14</sup>S. Glutsch, U. Siegner, M.-A. Mycek, and D. S. Chemla, *Phys. Rev. B* **50**, 17 009 (1994).
- <sup>15</sup>S. Glutsch, D. S. Chemla, and F. Bechstedt, *Phys. Rev. B* **51**, 16 885 (1995).
- <sup>16</sup>U. Siegner, M.-A. Mycek, S. Glutsch, and D. S. Chemla, *Phys. Rev. Lett.* **74**, 470 (1995).
- <sup>17</sup>C. Weisbuch and B. Vinter, *Quantum Semiconductor Structures: Fundamentals and Applications* (Academic, San Diego, 1991).
- <sup>18</sup>T. Yajima and Y. Taira, *J. Phys. Soc. Jpn.* **47**, 1620 (1979).
- <sup>19</sup>A. M. Weiner, S. De Silvestri, and E. P. Ippen, *J. Opt. Soc. Am. B* **2**, 654 (1985).
- <sup>20</sup>Note that the generation of frequency-shifted coherent emission by the process discussed by Ahn *et al.*, *Phys. Rev. Lett.* **82**, 3879 (1999), can be excluded for our experiments due to the well-resolved decay of the FWM traces in Fig. 3(b).
- <sup>21</sup>W. H. Hesselink and D. A. Wiersma, *Phys. Rev. Lett.* **43**, 1991 (1979).
- <sup>22</sup>K. Duppen, L. W. Molenkamp, and D. A. Wiersma, *Physica B* **127**, 349 (1984).